ACS OMEGA

Open Access

http://pubs.acs.org/journal/acsodf

Article

Synthesis, Properties, and Biocompatibility of 4-Carboxyphenyboronic Acid-Modified Gelatin-Methacryloyl: A Hydrogel for Retinal Surgeries

Hung-Da Chou, Chung-An Chen, Hao-Yu Liu, Shih-Jung Liu, Po-Liang Lai, Wei-Chi Wu, Yih-Shiou Hwang, Kuan-Jen Chen, Tsung-Ting Tsai,* and Chi-Chun Lai*

Cite This: *ACS Omega* 2024, 9, 42147−42158

Read Online

ACCESS | Metrics & More | Article Recommendations | Supporting Information

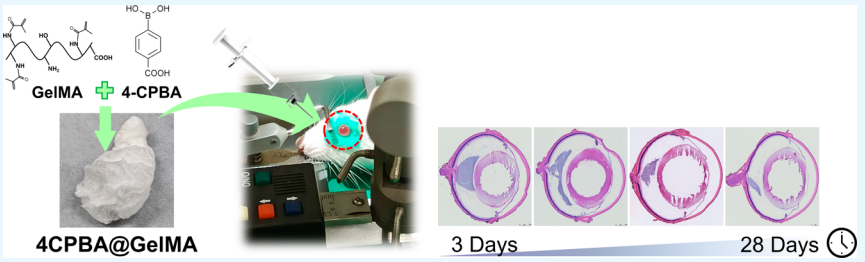

ABSTRACT: The current surgical adjunctive for vitreoretinal surgeries fails to provide an adequate 3D structure for cellular regeneration. A one-pot synthesis of gelatin-methacryloyl (GelMA) followed by modification with 4-carboxyphenylboronic acid (4-CPBA) was performed to fabricate 4-CPBA-modified GelMA (4CPBA@GelMA), a gelatin-based hydrogel. 4CPBA@GelMA was photo-cross-linked by 405 nm violet light and examined using nuclear magnetic resonance (NMR), Fourier-transform infrared spectrometry (FTIR), scanning electron microscopy (SEM), and rheometry. In vitro biocompatibility was examined by Müller cell proliferation assays exposed to 4CPBA@GelMA and violet light. In vivo retinal biocompatibility was evaluated by electroretinography of rat eyes that were exposed to intravitreally injected and photo-cross-linked 4CPBA@GelMA at days 3, 7, 14, and 28 post-injection. Following electroretinography, histology and immunohistochemistry were performed on the retinas. The NMR results indicated amidation of GelMA by 4-CPBA, and FTIR confirmed the presence of the CPBA ring in 4CPBA@GelMA samples. SEM revealed that 4CPBA@GelMA had significantly larger pores than GelMA (56.9 ± 9.5 vs 35.1 ± 2.8 μm; $P < 0.001$). Rheological findings showed that, unlike GelMA and gelatin, 4CPBA@GelMA has Newtonian fluid properties at room temperature. Exposure to 4CPBA@GelMA did not significantly affect Müller cell viability in a proliferation assay; moreover, electroretinography findings indicated normal waveforms and implicit times, and histology and immunohistochemistry examinations revealed no significant changes. In this study, we established the high retinal compatibility of 4CPBA@GelMA. The low viscosity of 4CPBA@GelMA is ideal for injection via small-gauge needles, and the larger pore size and three-dimensional network both potentiate cellular migration and growth. These features made 4CPBA@GelMA a candidate for vitreoretinal surgical adjunctive that might promote retinal regeneration.

1. INTRODUCTION

A full-thickness macular hole (FTMH) with or without retinal detachment is a defect in the most important part of the neurosensory retina. Failure to close the hole in time will have profound effects on visual acuity.[1] The mainstay treatment for a macular hole is surgical, generally involving a vitrectomy to clear the pathological vitreous humor and additional internal limiting membrane (ILM) peeling to promote hole closure. After peeling of the ILM, an inverted ILM flap may be created to cover the hole and aid hole healing.[2] This ILM flap was found to provide a scaffold for the Müller cells to migrate toward the center of the hole and increase the production of neurotrophic factors, which in turn promotes the migration of the Müller cells.[3−5]

The additional surgical step of creating and stabilizing the inverted ILM flap is technically challenging. It requires careful manipulation of the created flap to position it in the ideal location. Several other grafts have been demonstrated to promote FTMH healing but face similar surgical challenges.[6] To overcome this, surgical adjunctives can be utilized to stabilize the positioned flap intraoperatively and post-

Received: March 24, 2024
Revised: September 19, 2024
Accepted: September 25, 2024
Published: October 1, 2024

operatively and can assist with healing.[7] Various surgical adjunctives have been proposed, including autologous blood clots, autologous platelet concentrates, and ophthalmic viscosurgical devices (OVDs).[8−10]

Although these surgical adjunctives have been shown to improve outcomes, they have disadvantages. The autologous blood and platelet concentrates must be extracted from the patient during the vitrectomy procedure and processed immediately; sterilization is challenging and time-consuming. The OVD gel has been demonstrated in our previous studies to facilitate surgeries; however, the OVD gel may be washed away soon after application. Furthermore, none of the current adjunctives can provide a scaffold to facilitate tissue healing. Thus, new surgical adjunctives are necessary.

Gelatin is derived from collagen and is one of the most investigated polymers found in nature. Gelatin dissolves in hot water and spontaneously forms gels with a three-dimensional (3D) network upon cooling. This property has led to its use for preparing hydrogels, which can retain water and dissolved materials in a gel state instead of as a liquid. These hydrogels are extensively used in biomedical applications, including for drug delivery and to provide a supportive environment for cell growth.[11,12] Gelatin hydrogels transition to solution between 20 and 30 °C. Although this temperature is affected by the gelatin's molecular weight,[13] at normal human body temperature (37 °C), the hydrogel becomes liquid. To maintain the gel state at body temperature for various applications, cross-linking modifications are often required to create covalent bonds, such as chemical cross-linking by glutaraldehyde, transglutaminase, or genipin.[13,14]

Alternatively, cross-linking by light (i.e., photo-cross-linking) has been employed in some hydrogel approaches to maintain structural integrity at high temperatures.[15,16] Photo-cross-linking has numerous advantages, such as enabling spatiotemporal control over the behavior of the reaction, being highly efficient, and resulting in minimal byproducts.[17] Gelatin can be modified with methacrylamide and methacrylate groups to produce a gelatin-methacryloyl (GelMA) hydrogel that becomes photopolymerizable after mixing with a photoinitiator. Rapid cross-linking can occur in GelMA upon exposure to light with a wavelength appropriate for the added photoinitiator.[18,19] This unique property enables the control of GelMA's mechanical properties, making it suitable for various applications, including 3D cell culturing and tissue engineering.[20,21] Additionally, it has been demonstrated that GelMA can achieve in situ gel formation and provide long-term triamcinolone delivery after injection into the eye.[22]

A recent study proposed further modifying GelMA by integrating reversible covalent bonds, such as boronic ester, disulfide, or Schiff-base bonds.[23] Adding boronic ester bonds, such as 4-carboxyphenylboronic acid (4-CPBA), prompts the 3D network within the 4-CPBA-modified GelMA (4CPBA@GelMA) to reorganize, providing a more suitable 3D microenvironment for tissue regeneration.[24] The mechanical scaffold that could facilitate cell proliferation and the drug delivery potential of the hydrogel both made 4CPBA@GelMA a surgical adjunctive candidate. In this study, we investigated the properties of 4CPBA@GelMA and focused on its toxicity to the retina in order to establish a foundation for applying this material in ophthalmology.

2. EXPERIMENTAL SECTION

2.1. Chemicals and Reagents. Gelatin from porcine skin, *N*-hydroxysuccinimide (NHS), *N*-(3-(dimethylamino)propyl)-*N*′-ethylcarbodiimide hydrochloride (EDC), 4-CPBA, dimethyl sulfoxide (DMSO), sodium bicarbonate, sodium carbonate, methacrylic anhydride (MAA), glycine, deuterium oxide (D_2O), and 2,4,6-trinitrobenzenesulfonic acid (TNBS) solution (5 w/v% in H_2O solution) were purchased from Sigma-Aldrich (St. Louis, MI, USA). HCl, sodium dodecyl sulfate (SDS), and NaOH were purchased from J.T. Baker (Phillipsburg, NJ, USA). Lithium phenyl (2,4,6-trimethylbenzoyl) phosphinate (LAP) was purchased from TCI (Tokyo, Japan).

Slide-A-Lyzer dialysis cassettes (irradiated, 10K MWCO) were purchased from Thermo Fisher Scientific (Cleveland, OH, USA). A Millex-HA Filter Unit for a 33 mm-diameter sterile syringe filter with a 0.45 μm pore size mixed cellulose ester membrane was purchased from Merck (Darmstadt, Germany). Dulbecco's phosphate-buffered saline, Dulbecco's modified Eagle's medium: nutrient mixture F12 (DMEM/F12), fetal bovine serum (FBS), phosphate-buffered saline (PBS), and penicillin−streptomycin were purchased from Gibco (Grand Island, NY, USA). Double-distilled water was obtained with an Arium Advance Pure Water System (Sartorius, Göttingen, Germany); it was prepared using a minimum resistivity of 18.2 MΩ·cm.

2.2. GelMA and 4CPBA@GelMA Synthesis. Gelatin was modified with MAA by using an alkalic buffer solution per the method of Shirahama et al.[14] In brief, the gelatin (type A, 175 bloom) was dissolved in carbonate−bicarbonate (CB) buffer (250 mM, pH = 9) and stirred homogeneously at 50 °C. Subsequently, MAA (0.1 mL per gram of gelatin concentration at 10 w/v%) was added to the gelatin solution under magnetic stirring at 500 rpm for 3 h, and the pH was then readjusted to 7.4 with 6 N HCl to stop the reaction. After filtration, dialysis in the Slide-A-Lyzer cassettes, and lyophilization, the GelMA samples were stored at −20 °C until further use.

4CPBA@GelMA was synthesized by modifying GelMA with 4-CPBA through an NHS/EDC-mediated carbodiimide cross-linking reaction following Xie et al.[24] First, 1.0 g of GelMA was dissolved in 50 mL of pure water in a 45 °C bath. Simultaneously, 0.8 g of 4-CPBA, 2.0 g of NHS, and 3.0 g of EDC were dissolved in 30 mL of DMSO for 2 h for activation. The activated 4-CPBA solution was then added dropwise to the GelMA water solution, and the reaction proceeded for 16 h in a 37 °C oven environment. The product was dialyzed in a dialysis bag (molecular weight cutoff of 12−14 kDa, Rainbow Biotechnology, Taipei, Taiwan) for 4−5 days to remove the byproducts; it was then freeze-dried for 3 days to obtain a foam-like powder.

2.3. Fabrication of a Photo-Cross-Linking Device and Mixing the Hydrogel with a Photoinitiator. To deliver the light for photo-cross-linking, a homemade device was printed using a 3D printer (Ender-3 V2 3D, Creality 3D, Shenzhen, China) with polylactic acid (Figure S1). A modular 405 nm violet-light-emitting diode (LED) was mounted on the device by tenoning.

To prepare the hydrogel for photo-cross-linking, the 4CPBA@GelMA was dissolved in pure water to prepare a 20% stock solution. Next, 1% LAP as a photoinitiator solution was added into 4CPBA@GelMA at a 1:1 ratio in a centrifuge tube, and the working solution (10% 4CPBA@GelMA with

https://doi.org/10.1021/acsomega.4c02842
ACS Omega 2024, 9, 42147−42158

0.5% LAP) was mixed in a vortex mixer for 30 s before placing it in a dry bath incubator set to 40 °C for at least 10 min. This hydrogel-LAP photoinitiation mixture had a sol−gel transition 2 min after exposure to 405 nm violet light.

2.4. Nuclear Magnetic Resonance, Fourier-Transform Infrared Spectrometry, and Scanning Electron Microscopy. To verify the substitution, ^{1}H nuclear magnetic resonance (NMR) spectroscopy was performed as previously described.[14,24] Gelatin, GelMA, and 4CPBA@GelMA samples were separately dissolved at approximately 20 mg/mL in deuterium oxide. The chemical shift of each sample was measured at 37 °C and analyzed with a 600 MHz NMR spectrometer (AVANCE III HD 600, Bruker, Switzerland). The compositions of the gelatin, GelMA, and 4CPBA@GelMA samples were recorded with a Fourier-transform infrared spectroscopy (FTIR) device (Nicolet iS 5; Thermo Scientific, Waltham, MA, USA) between 4000 and 400 cm^{-1} by using its attenuated total reflection mode at room temperature.

The scanning electron microscopy (SEM) images were used to compare the microstructures of the cross-linked GelMA and 4CPBA@GelMA hydrogels.[25,26] After mixing with LAP, photo-cross-linking was performed by exposing the hydrogels to 405 nm violet light for 2 min. The samples were then frozen for 2 days at −80 °C, followed by freeze-drying at −50 °C for 3 days to obtain foamy fragments. The samples were sputter-coated with a layer of platinum particles before the photographs were taken within high vacuum mode at 10 kV for field emission SEM (Hitachi SU8220, Tokyo, Japan). The pore size of the hydrogels was calculated from five randomly selected SEM photographs using ImageJ software (National Institutes of Health, USA). The P value was calculated using Student's t-test.

2.5. Determination of the Degree of Functionalization. To quantify the degree of functionalization (DoF), a TNBS assay was performed with the technique used by Habeeb et al.[27] and modified by Shirahama et al.[14] In brief, GelMA and gelatin samples were separately dissolved in sodium bicarbonate buffer (0.1 M, pH = 8.5) at a concentration of 1.6 mg/mL. Each solution was then mixed with 0.2% TNBS solution (in 0.1 M sodium bicarbonate buffer); both solutions were 250 μL and then incubated at 37 °C for 3 h. Next, 250 μL of 10% (w/v) SDS and 125 μL of 1 M HCl were added to each solution to stop the reaction. The absorbance of each sample was measured at 335 nm. The glycine standard curve was then plotted to determine the concentration of the amino group; sample solutions were prepared at 0, 0.8, 8, 16, 32, and 64 μg/mL.

2.6. Rheological Analysis, Transparency and Swelling Properties, and Degradation In Vitro. The mechanical properties of the gelatin, GelMA, and 4CPBA@GelMA hydrogels were characterized by an MCR 302e rheometer (Anton Paar Physica, Ostfildern, Germany) with the PP25 measuring parallel plate accessory. The cylinder was measured with P-PTD220 Air and C-PTD 200 heating rheometer systems. The experimental conditions for gelatin and GelMA were as follows: 2% shear strain with a 1 Hz frequency at a temperature between 20 and 37 °C, 0.01 to 1000% shear strain with a 10 s^{-1} angular frequency at 20 °C for the amplitude sweep, and 0.1 to 100 s^{-1} shear rate at 20 °C for the flow curve. The experimental conditions for 4CPBA@GelMA were as follows: 2% shear strain with a 1 Hz frequency at a temperature between 4 and 37 °C, 0.01 to 1000% shear strain with a 10 s^{-1} angular frequency at 4 °C for the amplitude sweep, and 0.1 to 100 s^{-1} shear rate at 4 °C for the flow curve.

Transparency was tested using the GelMA and 4CPBA@GelMA samples after photo-cross-linking to compare the visibility and color of the letters on the white paper. The swelling property was examined using the photo-cross-linked lyophilized and nonlyophilized samples, which generated two respective swelling ratios. The initial weight of the samples was recorded (W_0), and again after the samples were immersed in 1× PBS (pH 7.4) at room temperature for 24 h (W_t). The swelling ratio was calculated by 1[24,28,29]

$$\text{swelling ratio } (\%) = (W_t - W_0)/W_0 \times 100\% \quad (1)$$

For the in vitro degradation examination, the weight of the freeze-dried hydrogel samples (∼300 μL) was measured and recorded as M_0. Then, the hydrogel samples were immersed in 1× PBS (pH 7.4) and placed in an oven maintained at 37 °C. At different time points, they were removed from the oven, washed with pure water, lyophilized, and recorded as M_t. The degradation rate was determined using formula 2[24]

$$\text{degradation rate } (\%) = (M_0 - M_t)/M_0 \times 100\% \quad (2)$$

2.7. Cell Line and Animals. The study was performed in accordance with the ethical standards of the 1964 Declaration of Helsinki. Professor Vijay Sarthy (Northwestern University, Evanston, IL, USA)[30] kindly provided the rat Müller cells (rMC-1; #RRID: CVCL_8140). The cells were cultured with DMEM/F12 containing 10% FBS, penicillin−streptomycin, and 2 mM L-glutamine.

Sprague−Dawley rats were used in the current study, and all experimental procedures were in accordance with the Association for Research in Vision and Ophthalmology (ARVO) Resolution on the Treatment of Animals in Research. The animal protocol was approved by the Institutional Animal Care and Use Committee of Chang Gung University (no. 2020121501). The rats were maintained in a 12/12 h light−dark cycle. All surgeries were performed under sodium pentobarbital anesthesia unless otherwise specified, and all efforts were made to minimize suffering.

2.8. Cellular Proliferation and Adhesion Assays. To investigate the impact of 405 nm violet light and 4CPBA@GelMA on rMC-1, we performed a 2,5-diphenyl-2H-tetrazolium bromide (MTT) assay with a cell counting kit-8 (CCK-8; Sigma-Aldrich, Budapest, Hungary). 96-well plates were filled with culture medium DMEM/F12 containing 10% FBS. In each plate, 1 × 10^4 Müller cells were seeded and allowed 24 h to proliferate and then rinsed with PBS; the excess solution was removed.

Subsequently, the cells were divided into control groups and three experimental groups. For the LAP only group, 20 μL of 0.5% LAP was added to each plate; for the 4CPBA@GelMA only group, 20 μL of 4CPBA@GelMA-LAP mixture was added to each plate; and for the 4CPBA@GelMA with violet light experimental group, the plates were further exposed to violet light with the aforementioned homemade LED device (Figure S1) for 2 min. The control group was not exposed to violet light, LAP, or 4CPBA@GelMA.

After these procedures, 10 μL of CCK-8 and 90 μL of culture medium (10% FBS and DMEM/F12) were added to each plate, and the plates were incubated for 1 h inside a humidified incubator for the CCK-8 to be cleaved by the mitochondrial dehydrogenase of the alive Müller cells. The cleaved CCK-8 formed formazan dye, which was quantified by

https://doi.org/10.1021/acsomega.4c02842
ACS Omega 2024, 9, 42147−42158

Scheme 1. Overview of the Synthesis of 4CPBA@GelMA Hydrogel and the Biocompatibility Examination in a Rodent Model (GelMA, Gelatin-methacryloyl; MAA, Methacrylic Anhydride; 4-CPBA, 4-Carboxyphenyboronic Acid; 4CPBA@GelMA, 4CPBA-Modified GelMA)

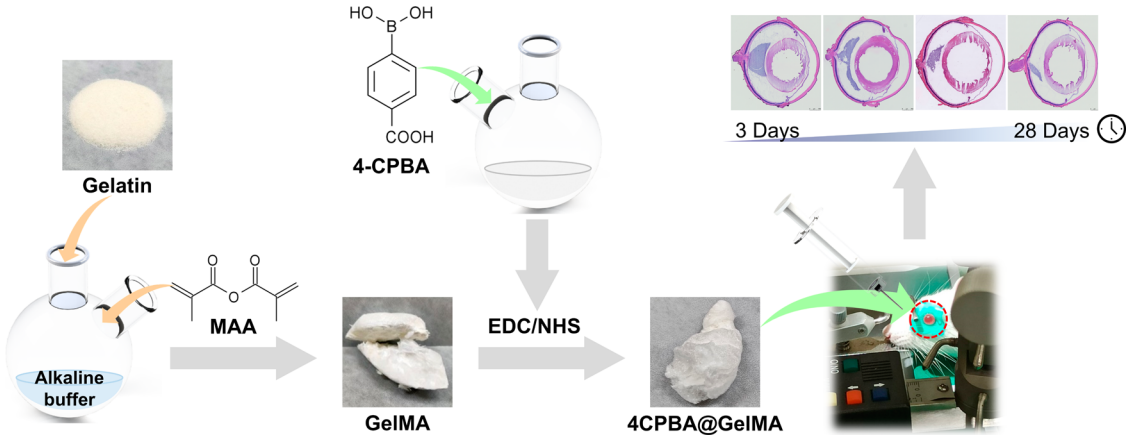

an immunosorbent assay reader (VERSAmax, Molecular Devices, Sunnyvale, CA, USA); the optical density was calculated against a background control. Six replicates were performed for each group.

The cell adhesion assay was modified from the study by Teshima et al.[31] Briefly, 120 μL of 4CPBA@GelMA hydrogel solution (10%) containing 0.5% LAP was prepared in a 48-well tissue culture plate. After 2 min of photo-cross-linking, the hydrogels were washed with 1× PBS thrice. Human Müller cells (1×10^5 cells) were seeded at 37 °C under 5% CO_2 for 24 h in 300 μL of GlutaMAXTM DMEM medium supplemented with 50 U/mL penicillin, 50 g/mL streptomycin (Invitrogen-Gibco-Life Science Technology, Karlsruhe, Germany), and 10% FBS. After incubation, we used an optical microscope (Olympus CKX31, Tokyo, Japan) to directly observe cellular adhesion and take photographs for documentation.

Data from the assays were analyzed using Excel for Mac (version 16.7; Microsoft, Redmond, WA, USA). Continuous variables were compared using an independent *t*-test, and a *P* value of less than 0.05 was considered statistically significant.

2.9. Intravitreal Injection of 4CPBA@GelMA and Photo-Cross-Linking. After 4CPBA@GelMA was mixed with LAP as aforementioned, the photopolymerizable hydrogel was injected into the vitreous cavity of the eyes of the rats through the pars plana by using a 1 mL syringe and a 32-gauge needle at room temperature. After the needle was advanced to approximately 3−4 mm inside the eye, 5 μL of the hydrogel was slowly injected. The needle was then withdrawn, and the fundus reflex was checked for any vitreous hemorrhage.

Immediately after the intravitreal injection, the eyes were exposed to violet light with the homemade LED for 2 min to complete the photo-cross-linking. For the violet-light-exposure-only group, violet light was emitted at the eyes for 5 min without injecting the hydrogel. One eye from each rat was used for the above experiments.

2.10. Electrophysiology Examinations. To evaluate the functional changes of eyes exposed to 405 nm violet light and 4CPBA@GelMA, electroretinograms (ERGs) were performed for each rat at 7,14, and 28 days post-injection. Both eyes of each rat were examined separately with an ERG recording system (RETIport 32 Version 4.7.2.8: Roland Consult, Brandenburg, Germany). The rats were subjected to adaptation overnight in a dark room before being anesthetized using xylazine hydrochloride (12.5 mg/kg) and a mixture of tiletamine HCl and zolazepam HCl (50 mg/kg). The pupils were then dilated with topical 1.0% atropine sulfate, and the corneas were kept lubricated with Viscoat OVD (Alcon, Fort Worth, TX). Contact lenses with attached LEDs were then placed in both eyes. Reference and ground electrodes were fixed subdermally between the eyes and at the base of the tail, respectively. Scotopic and photopic ERGs were recorded with a standard white flash (3 cd·s/m2 with a duration of 10 ms) inside a light-proof darkroom.

2.11. Histology and Immunohistochemistry Examinations. At day 3 post-injection, the eyes underwent enucleation directly without ERG examination. At days 7, 14, and 28 post-injection, the eyes were enucleated after ERG. The enucleated eyeballs were soaked in cryomolds containing the optimal cutting temperature compound. Approximately 20 cryosections of 10 μm in thickness were sliced by following the corneal apex-optic nerve center axis. The cryosections were then fixed with 4% paraformaldehyde at room temperature.

Hematoxylin and eosin (H&E) stains were used for histological examinations. For immunohistochemistry examinations, permeabilized cryostat sections were prepared by soaking the sections with 0.1% TritonX-100 (T8787; Sigma-Aldrich St. Louis, MO, USA) for 15 min at room temperature and then washed with 1× PBS three times. Next, all cryosections were blocked with 1% bovine serum albumin (A7030, St. Louis, MO, USA) in PBS for 30 min in a humidified chamber at room temperature before the administration of primary antibodies interleukin-6 (IL-6) and tumor necrosis factor-alpha (TNF-α) (#GTX110527 and #GTX110520, respectively; Gene Tex, Arvine, CA, USA) overnight at 4 °C. Fluorescent probes (Alexa Fluor 488 Goat anti-Rabbit IgG[H + L], #A11088, 1:1000, Invitrogen, USA) were then applied for 2 h at room temperature. The cells were again washed three times with PBS, and the nuclei were then costained with 4,6-diamidino-2-phenylindole (DAPI; Sigma-Aldrich, Budapest, Hungary). Images of the cryosections were taken with a microscope-mounted camera (DP74 mounted on BX60; Olympus, Tokyo, Japan) and processed with commercial software (cellSens standard ver. 2.3; Olympus); the images were merged with the ImageJ software.

https://doi.org/10.1021/acsomega.4c02842
ACS Omega 2024, 9, 42147−42158

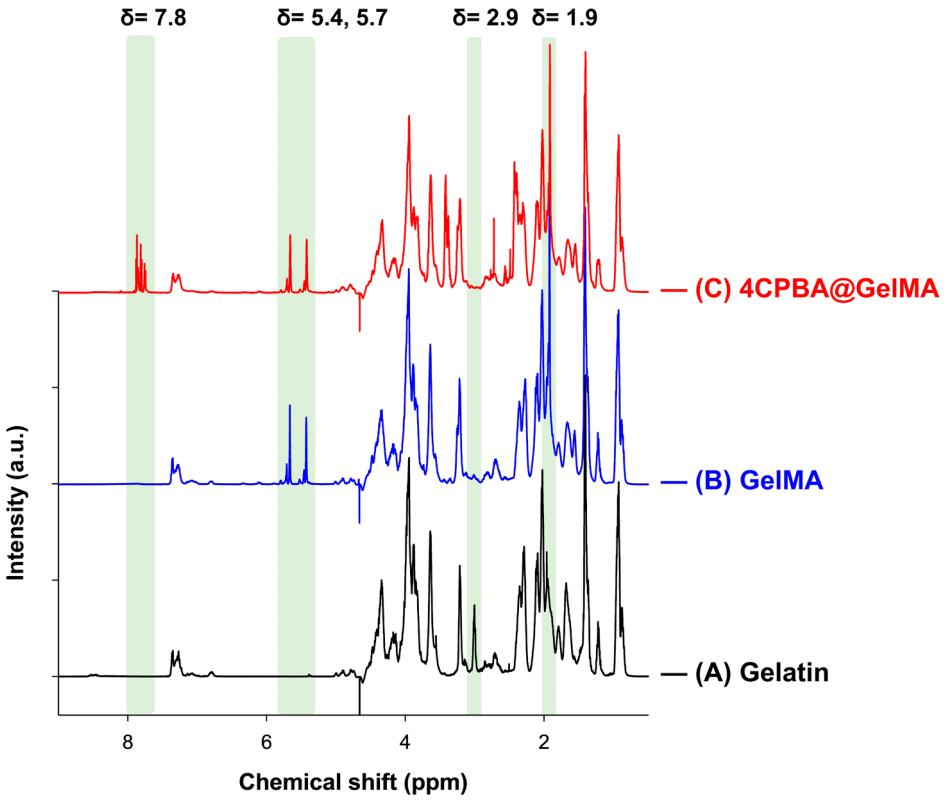

Figure 1. NMR spectra of (A) gelatin, (B) GelMA, and (C) 4CPBA@GelMA recorded in D_2O at 37 °C in nuclear Overhauser effect mode.

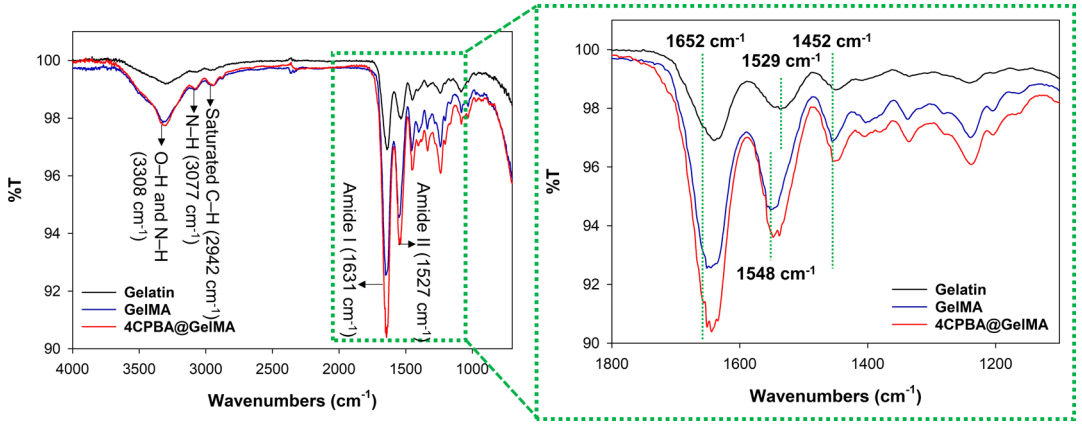

Figure 2. FTIR spectra of gelatin, GelMA, and 4CPBA@GelMA measured at room temperature in attenuated total reflection mode.

3. RESULTS AND DISCUSSION

An overview of the synthesis of 4CPBA@GelMA and the intraocular biocompatibility examination is shown in Scheme 1. A one-pot GelMA synthesis was modified by gelatin and MAA from a simple and efficient CB buffer system to acquire a high-quality compound, which was further modified by 4-CPBA to acquire the final product of 4CPBA@GelMA. In this study, we used DMSO instead of dimethylformamide due to its toxic effects, including gastric irritation, skin eruption, and hepatotoxicity.[32] The NMR and FTIR results demonstrated that our homemade GelMA and 4CPBA@GelMA compounds were successfully synthesized. In order to confirm the biocompatibility of this vitreoretinal surgical adjunctive candidate, we conducted in vitro Müller cell proliferation and adhesion assays and in vivo electrophysiology, histology, and immunohistochemistry examinations at 3, 7, 14, and 28 days after intravitreal injection of 4CPBA@GelMA in a rodent model.

3.1. NMR and DoF. The ^{1}H NMR spectroscopy of gelatin, GelMA, and 4CPBA@GelMA was obtained, the methacrylation was characterized, and the DoF of the gelatin chains was quantified (Figure 1). The methacrylate vinyl group signals at 5.4 and 5.7 ppm correspond to acrylic protons of the methacrylamide group and to the same in the hydroxylysine residues, respectively.[33] These twin peaks were present in the NMR spectra of 4CPBA@GelMA and GelMA but were absent in the gelatin. Furthermore, an increased signal at 1.9 ppm corresponding to methyl protons of methacryloyl groups is visible in the 4CPBA@GelMA and GelMA results but not in those for the gelatin samples.

The lysine signal at 2.9 ppm corresponding to methylene protons of the unreacted lysine groups was absent for

https://doi.org/10.1021/acsomega.4c02842
ACS Omega 2024, 9, 42147−42158

4CPBA@GelMA and GelMA. In addition, we found a clear peak at 7.8 ppm in 4CPBA@GelMA. This peak corresponds to the aromatic hydrogens of the phenylboronic acid groups and confirms the successful amidation of GelMA by 4-CPBA.[24]

Typically, hydrogels with a high DoF have a higher modulus and slower degradation and are thus better able to maintain the long-term stability of the hydrogel in vivo,[34] which is a desired function for cell culture since this period will provide adequate time for the cells to migrate and proliferate within the hydrogel. In the current study, DoF can be calculated for the GelMA samples.[24,33] The NMR results (DoF = 92.83%) and TNBS assay (Table S1) revealed a high DoF for GelMA at over 90%, indicating the high stability and repeatability of the synthesis of GelMA. According to Xie et al.,[24] PBA groups in different PBA-gelatin could not be well quantified by NMR; thus, we were unable to determine the DoF in 4CPBA@GelMA.

3.2. FTIR and SEM. The specific vibration peaks of 3308 cm^{-1} (common signal for O−H and N−H stretching), 3077 cm^{-1} (N−H), 2942 cm^{-1} (saturated C−H stretching), 1631 cm^{-1} (amide I), and 1527 cm^{-1} (amide II) were observed for both gelatin and the synthesized GelMA and 4CPBA@GelMA (Figure 2).[35] The difference in the characteristic peaks of gelatin and GelMA/4CPBA@GelMA was at the second amide bond at 1529 cm^{-1}, which was shifted to 1548 cm^{-1} in GelMA and 4CPBA@GelMA.[36]

In addition, a peak at 1652 and 1452 cm^{-1} corresponding to the −CH═CH2− in GelMA was observed for both the GelMA and 4CPBA@GelMA but not for the gelatin samples.[23,37] Furthermore, in 4CPBA@GelMA, the prominent peak near 1652 cm^{-1} was likely due to the combination of this peak with the signal of C═C in the CPBA ring at 1650 cm^{-1}.[23,37] These peak features confirm the successful fabrication and chemical structures of GelMA and 4CPBA@GelMA.

The ideal gel for macular hole surgeries would act as a scaffold itself, without requiring other tissues to promote hole closure. Under SEM, we observed that both the GelMA and 4CPBA@GelMA had a 3D porous microstructure after lyophilization (Figure 3). Notably, the pore size was

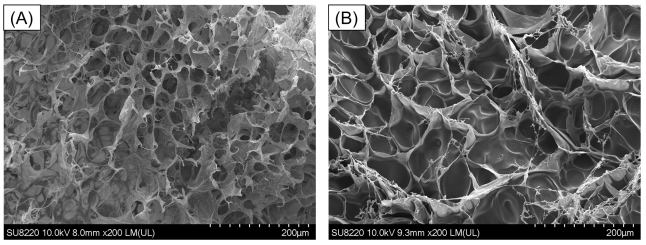

Figure 3. SEM images of the hydrogels. (A) GelMA had a significantly smaller porous microstructure compared with (B) 4CPBA@GelMA.

significantly smaller in GelMA (35.063 ± 2.826 μm) than in 4CPBA@GelMA (56.863 ± 9.452 μm) (n = 5; P < 0.001). According to Chen et al.,[23] the tighter packing of the molecules in 4CPBA@GelMA likely resulted in larger spaces (pores) in the gel. This larger porous microstructure is a desirable feature for the biofunction of hydrogels since it permits better permeability for nutrients and oxygen and allows cellular migration and intercellular interactions, thus potentially enhancing cell viability.[18,24] In addition, the 3D network of 4CPBA@GelMA may provide an excellent extracellular matrix-like environment for optimal macular hole restoration.

Furthermore, modification with boronic ester bonds, such as 4CPBA, relaxes the hydrogel structure and reorganizes the alignment of the gel matrix.[38] As a dynamic and reversible covalent bond, the boronic ester bond can slowly dissociate and provide a controlled release of the contents dissolved within the hydrogel.[23,24,38] Thus, by dissolving the needed materials in the tunable 4CPBA@GelMA, one may provide a well-balanced microenvironment for tissue regeneration.

3.3. Rheological Analysis, Transparency and Swelling Properties, and Degradation In Vitro. As shown in Figure 4A, the gelation (gel−sol transition) temperatures ($G' = G''$) for gelatin, GelMA, and 4CPBA@GelMA are 28.265, 26.176, and 9.690 °C, respectively, indicating that at room temperature of 20 °C, 4CPBA@GelMA is in liquid status but gelatin and GelMA are both in gel form. Under gel status, the shear stress of gelatin is higher at 1858 Pa, whereas GelMA and 4CPBA@GelMA are similar at 832.6 and 873.2 Pa, respectively (Figure 4B). The flow curve results show that under gel status, gelatin, GelMA, and 4CPBA@GelMA have shear-thinning properties with a yield point and are thus non-Newtonian fluids (Figure 4C). The above results conform with the properties of hydrogels.[39] Interestingly, when 4CPBA@GelMA is in a liquid state at 20 °C, it has a very low viscosity and is thus similar to a Newtonian fluid (Figure S2).

The rheological analysis described above revealed the low viscosity properties of 4CPBA@GelMA at room temperature. Compared with the widely used Viscoat OVD (Alcon; viscosity 40 000 mPa S) in ophthalmic surgery, the viscosity of 4CPBA@GelMA (∼5 mPa S) is much thinner at room temperature of 20 °C,[40,41] which is similar to water and thus can be easily injected without clogging the needle. This is especially relevant in retinal surgeries since the instruments are often 23 gauge or even 25−27 gauge in microincision vitrectomy. This increasingly narrower caliber of the surgical ports made the development of a gel that is thinner and easier to inject more critical. Furthermore, the watery property of 4CPBA@GelMA at room temperature has made the washout of the gel possible if the surgeon decides to redo or abort the gel application procedure. It is only after photo-cross-linking that 4CPBA@GelMA will become a more solid and stable mass and retain its desired position for an extended period.

The transparency test compared GelMA and 4CPBA@GelMA. Both hydrogels provide good transparency with clearly readable letters through the gel. GelMA appears slightly yellowish, whereas 4CPBA@GelMA is almost transparent (Figure S3). The swelling ratio of GelMA and 4CPBA@GelMA showed an 883.92 ± 24.32 and 842.5 ± 38.0% fluid retention/expansion rate of the lyophilized samples, respectively. This is in concordance with the other research; these swelling properties were relatively low, likely due to the denser cross-linked network structure.[28] Furthermore, we monitored the swelling property of cross-linked nondried hydrogels that were immersed in 1× PBS, and the results indicated that the 4CPBA@GelMA hydrogel would not only swell but also lose some weight (−10.20 ± 1.84% for GelMA and −11.14 ± 2.95% for 4CPBA@GelMA) (Table S2). These low swelling ratios implicate that once injected into the vitreous cavity, the hydrogels would not expand much and cause complications such as elevated intraocular pressure.[29]

The degradation of 4CPBA@GelMA is demonstrated in Figure S4. In the first week, a continuous degradation could be

https://doi.org/10.1021/acsomega.4c02842
ACS Omega 2024, 9, 42147−42158

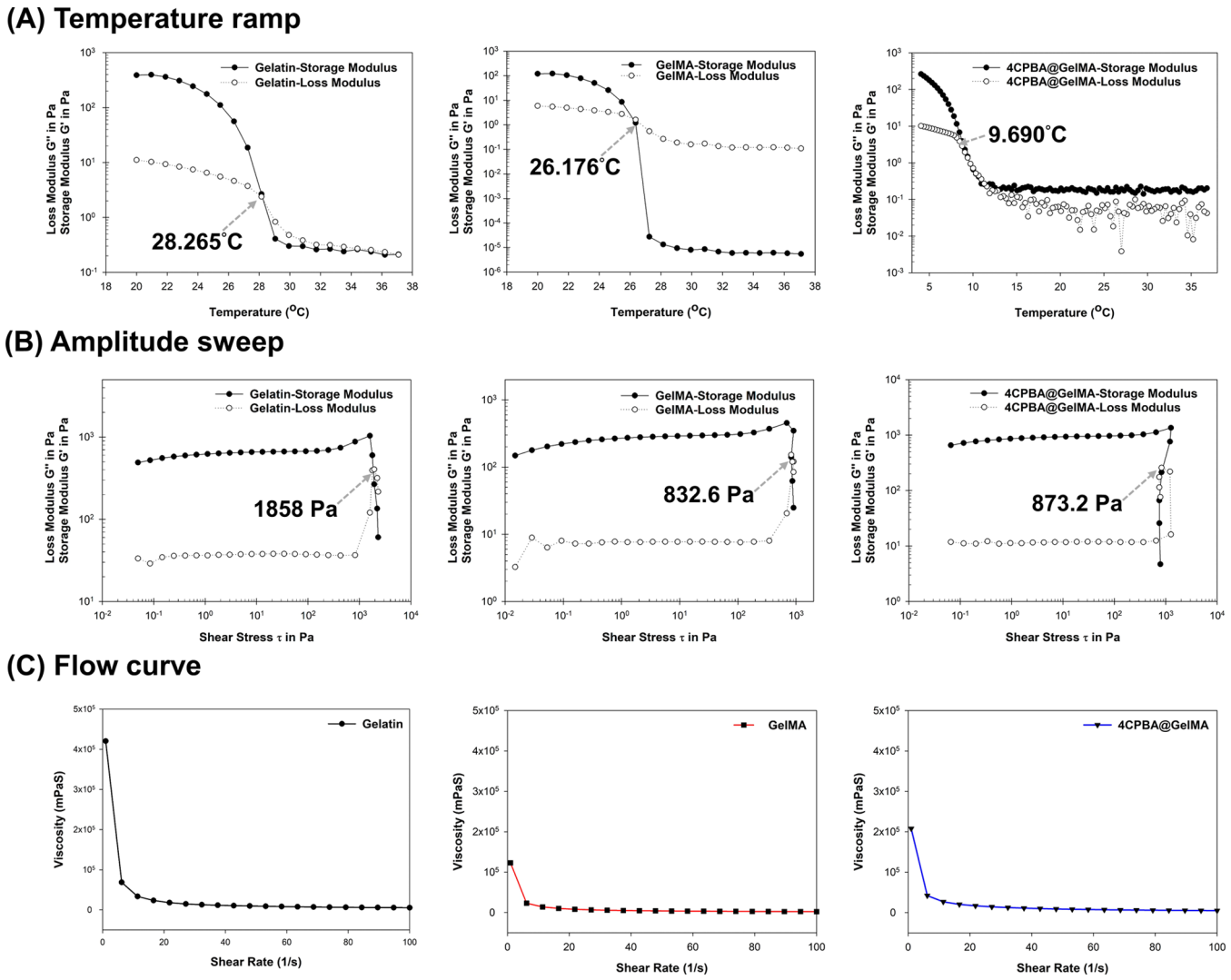

Figure 4. Rheological analysis of gelatin, GelMA, and 4CPBA@GelMA. Temperature ramp (A), amplitude sweep (B), and flow curve (C) are shown. The amplitude sweep and flow curve are examined while the hydrogels are in a gel form (20 °C for gelatin and GelMA; 4 °C for 4CPBA@GelMA).

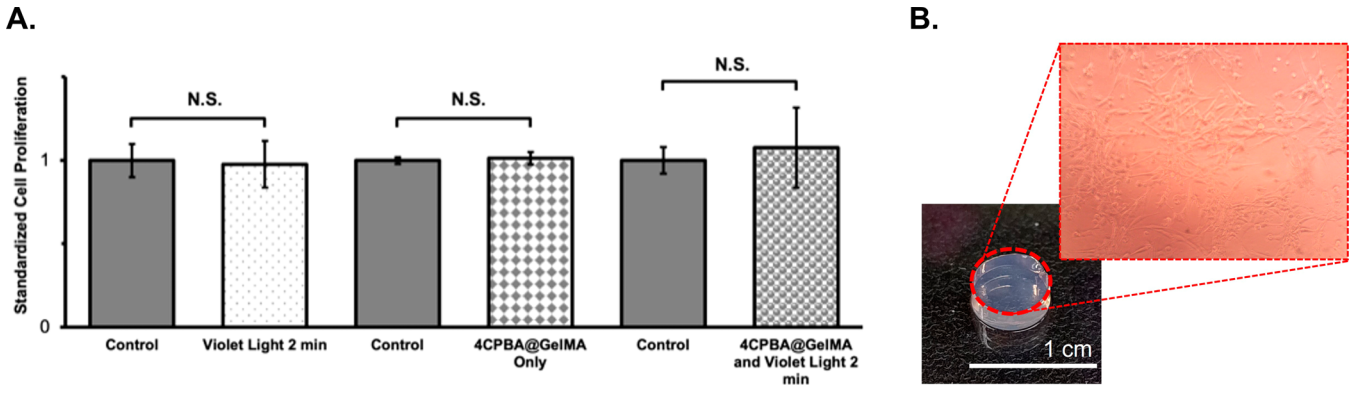

Figure 5. Viability and adhesive properties of Müller cells after exposure to violet light and 4CPBA@GelMA hydrogel. (A) Cell viability assays showed comparable cellular proliferation in the study and control groups at 6, 12, and 24 h (N.S. = nonsignificant; $n = 6$ in each group). (B) Müller cells adhered to the surface of 4CPBA@GelMA, displaying normal morphology.

observed; the process halted between days 7 and 28, with a residual weight ratio of around 50% at day 28. In addition, the degradation rate of GelMA in PBS solution without collagenase was very slow, according to the research from Wang et al.[42] The slow degradation of the 4CPBA@GelMA hydrogel enables its potential to act as a vehicle with slow drug-releasing capability.

https://doi.org/10.1021/acsomega.4c02842
ACS Omega 2024, 9, 42147−42158

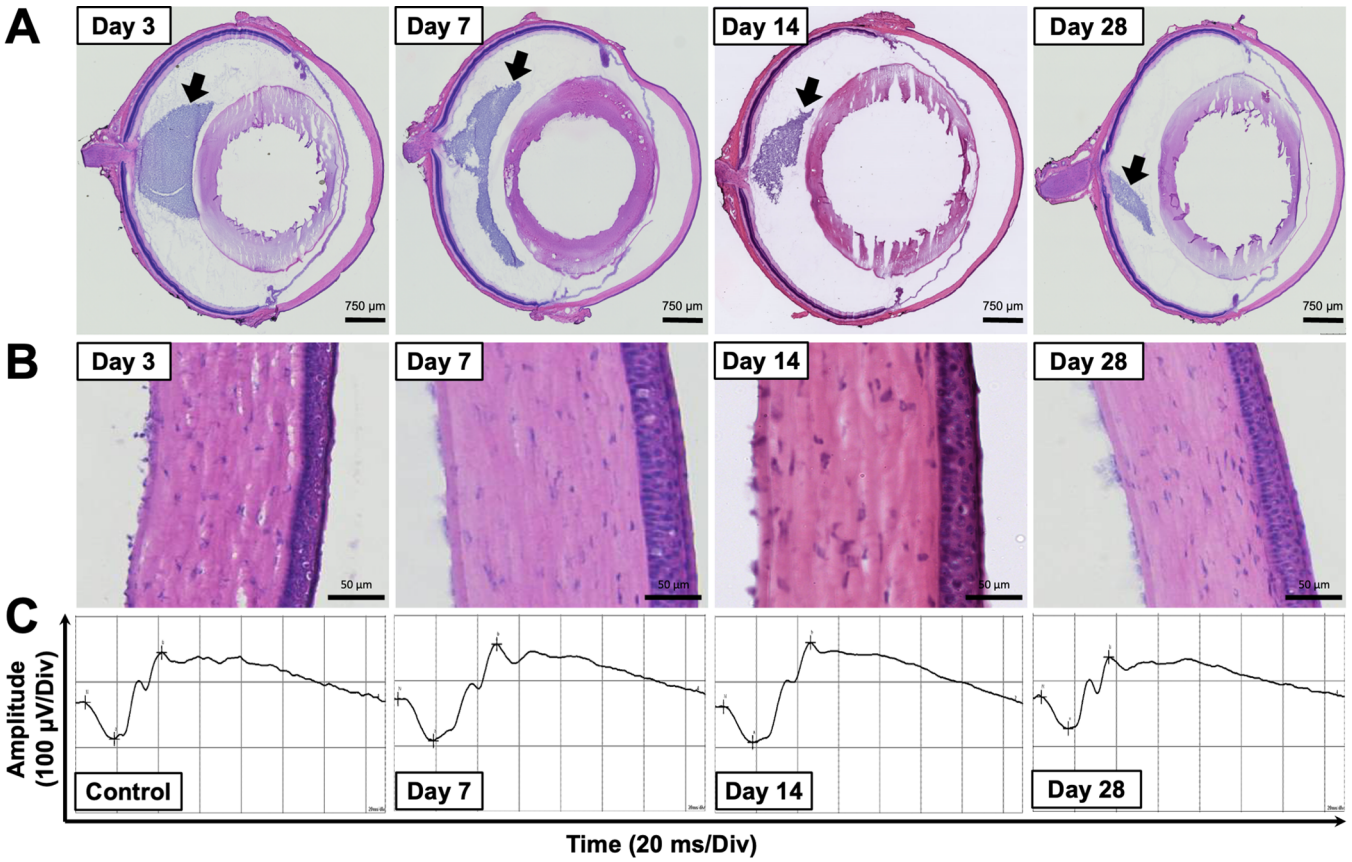

Figure 6. Serial histopathology and electroretinography of the eye after intravitreal 4CPBA@GelMA injection. (A) Micrographs showing the cross-section of the whole eye globe with the cornea to the right and the optic nerve stump to the left. The intraocular circular tissues are the crystalline lenses. The arrows indicate the injected 4CPBA@GelMA, which forms a condensed chunk adherent to the optic disc in the vitreous cavity that slowly dissolved (H&E stain). (B) Serial corneal histology sections showed normal morphology (H&E stain). (C) ERGs of the eyes before harvest, revealing normal a- and b-waves and implicit time. One representative ERG at post-injection day 7, 14, and 28 is shown, respectively. The control is a representative figure of the uninjected fellow eye at day 7 (Div, division.).

3.4. Müller Cell Viability and Adhesion upon Violet Light or 4CPBA@GelMA Exposure. To evaluate the toxicity of 4CPBA@GelMA and violet light exposure to the retina, rat Müller cells (rMC-a1) were exposed to 4CPBA@GelMA, and cell viability and adhesion were examined (Figure 5). For the cell viability at 6, 12, or 24 h, the results for the experimental groups were similar to those for the control group (all $P > 0.05$) (Figure 5A). We further evaluated the cellular adhesion properties to 4CPBA@GelMA. Figure 5B displays the morphology of the Müller cells cultured on the surface of the hydrogel at a common cell culture polystyrene plate for 24 h. The Müller cells stretched and adhered well without significant morphological alterations.

Together, these results suggest that violet light and 4CPBA@GelMA did not affect the viability or adhesive properties of Müller cells. The retina is a delicate and complex tissue with 10 histological layers and six major neuronal cell types. Although it is possible to interrogate retinal toxicity in more sophisticated retinal organoid models, these models are currently limited by extensive culture time and high cost.[43] We have chosen Müller cells to perform the in vitro studies since the Müller cells are thought to be the main cell type involved in the healing of a macular hole and are the primary and crucial cells in responding to other retinal injuries.[44,45]

3.5. Temporal Changes of 4CPBA@GelMA in the Vitreous Cavity. To investigate the eye morphology and in vivo change of 4CPBA@GelMA upon injection into the vitreous cavity, serial whole-eye histopathology was obtained on days 3, 7, 14, and 28 after intravitreal injection of 4CPBA@GelMA. The micrographs clearly demonstrate that condensed 4CPBA@GelMA stays inside the vitreous cavity and adheres to the optic disc. A slow dissolution was noted, but 4CPBA@GelMA remained at day 28 (Figure 6A). At the macroscopic level, the eyes were quiet, showed no signs of active inflammation, and the corneas and the crystalline lenses were clear before harvest. On the micrographs, no significant alterations were observed in the vital ocular structures, including the cornea, uvea, lens, retina, and optic nerve, and no retinal detachment was noted up to day 28 (Figure 6A,B). In addition, ERG was performed on the eyes before they were harvested for histopathology examinations on days 7, 14, and 28 after 4CPBA@GelMA injection (Figure 6C). The amplitude and the implicit time were unchanged compared with those of the controls.

These observations show that 4CPBA@GelMA did not cause morphological or functional harm to the eye when injected intravitreally; it also remained condensed, adherent to the optic disc, and slowly dissolved while persisting for up to 28 days. The electroretinography reflects the overall retinal circuitry and requires all of the neuronal cells to be intact to produce a normal result. The results of the assay assured the biocompatibility of 4CPBA@GelMA in the vitreous cavity.

https://doi.org/10.1021/acsomega.4c02842
ACS Omega 2024, 9, 42147−42158

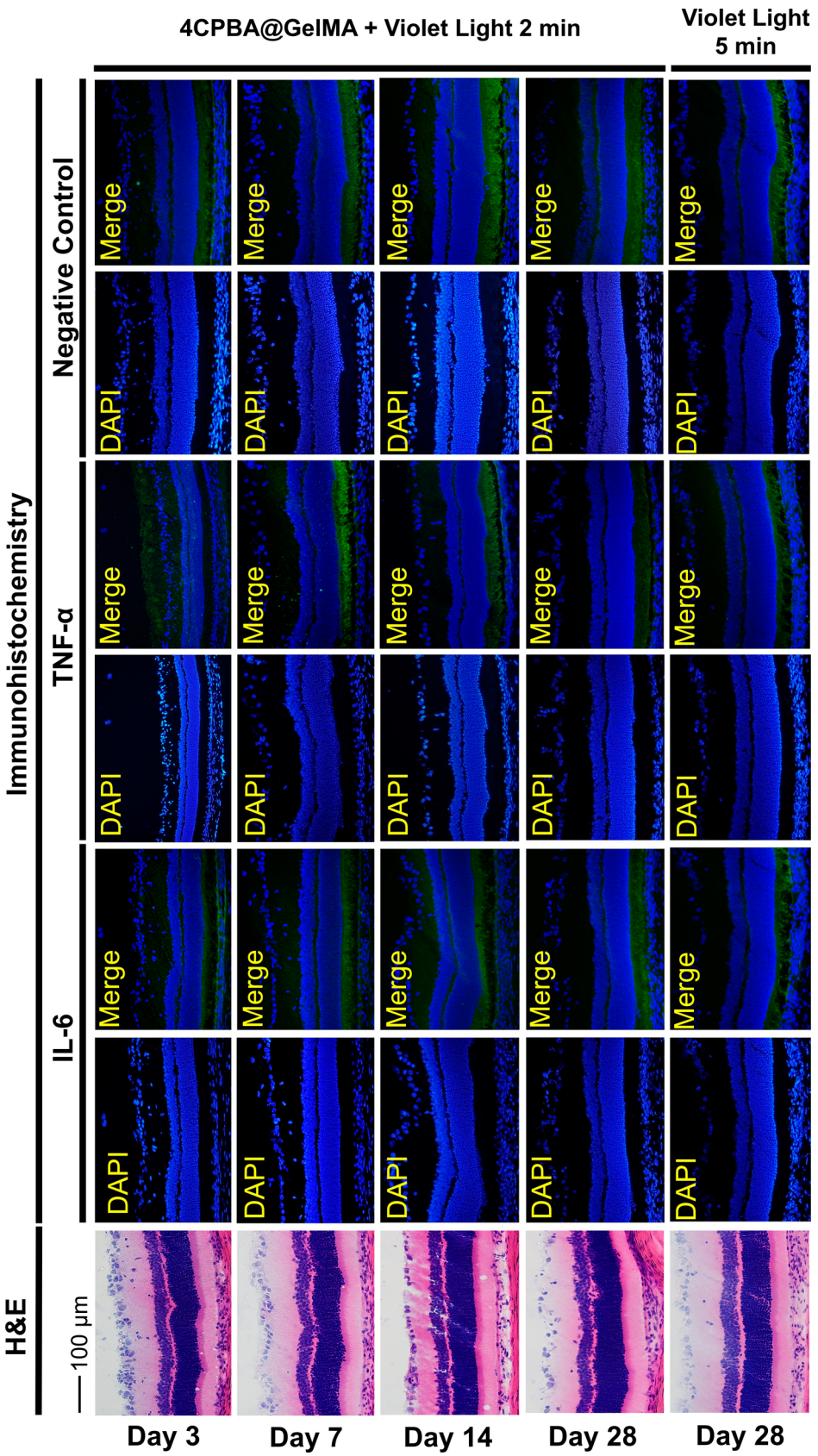

Figure 7. Serial histopathology and immunohistochemistry micrographs of retinas exposed to 4CPBA@GelMA with violet light photo-cross-linking or violet light only. The H&E micrographs reveal the retinal layers and the retinal pigment epithelium; these were morphologically unchanged in all groups. In the immunohistochemistry micrographs, the DAPI stain highlights the nuclei of the ganglion cells, the inner and the outer nuclear layers, and the retinal pigment epithelial layer. In the negative controls, some background fluorescence can be observed in the inner and outer segments of the photoreceptors. In the retinas stained by the inflammatory markers IL-6 and TNF-α, the fluorescence was comparable to the negative controls.

https://doi.org/10.1021/acsomega.4c02842
ACS Omega 2024, 9, 42147−42158

The slow degradation of the in vivo 4CPBA@GelMA can potentially achieve long-term delivery of drugs into the vitreous space. Various growth factors, including epidermal growth factor, fibroblast growth factor, somatomedin, and nerve growth factor, promote Müller cell migration or proliferation, which is the main biological process in the healing of a macular hole.[3,5] Recently, we also found that microRNA-152−3p and microRNA-196a-5p regulate Müller cell activities.[4] With 4CPBA@GelMA, the gel can be used to deliver the aforementioned agents directly into the hole area and release them slowly during the healing process, achieving an ideal functional healing instead of excessive scarring.[46]

3.6. Histopathology and Immunohistochemistry Examinations of the Retinas Exposed to 4CPBA@GelMA or Violet Light. The retina is a vital structure that is the closest tissue to the injected 4CPBA@GelMA; further histology and immunohistochemistry studies were performed to visualize the retinal changes (Figure 7). No significant structural alterations were observed on the H&E histology slides. Further IL-6 and TNF-α stains were used to highlight these inflammation markers. Background fluorescence was seen in the negative controls and was comparable to the fluorescence noted in the IL-6 and TNF-α groups. Faint immunostaining was noted in the ganglion cell and the inner plexiform layers in the TNF-α group on day 3; this was consistent with a previous report that barely detectable signals in the glial cell processes in the ganglion cell and the inner plexiform layers can be observed in control retinas.[47]

The above observations revealed no anatomical alterations or inflammatory biomarkers in the retinas that had been exposed to 4CPBA@GelMA. It is desired that the intraocularly injected material does not elicit any inflammatory response since any such reaction can cause vision deterioration and might lead to long-term sequela. The retinal changes after exposure to violet light were independently examined and were unremarkable. In fact, as opposed to UV light, which may harm the eye, violet light has been suggested to prevent myopia progression.[48] This further supports our choice to use violet-light-activated LAP as the photoinitiator instead of the other UV light-activated photoinitiators.

4. CONCLUSIONS

We modified the photopolymerizable GelMA hydrogel with 4-CPBA boronic ester bonds by DMSO and created 4CPBA@GelMA, which is a low-viscosity Newtonian hydrogel that can be easily injected. 4CPBA@GelMA has a network with large porous structures; this may promote 3D cellular growth and can release dissolved materials slowly. Biocompatibility evaluations of 4CPBA@GelMA in Müller cells and retinas provide a basis for further exploration of the application of 4CPBA@GelMA in vitreoretinal surgeries.

■ ASSOCIATED CONTENT

Supporting Information

The Supporting Information is available free of charge at https://pubs.acs.org/doi/10.1021/acsomega.4c02842.

DoF of GelMA by the TNBS assay, effects of swelling ratio of 4CPBA@GelMA, 3D printed device with a mounted LED for photo-cross-linking, rheological analysis of 4CPBA@GelMA flow curve, transparency of GelMA and 4CPBA@GelMA, and degradation rate of 4CPBA@GelMA hydrogel in vitro test for this study (PDF)

■ AUTHOR INFORMATION

Corresponding Authors

Tsung-Ting Tsai − *Department of Orthopaedic Surgery, Spine Section and Bone and Joint Research Center, Chang Gung Memorial Hospital, Taoyuan 333, Taiwan; School of Medicine, Chang Gung University, Taoyuan 333, Taiwan;* Email: tsai1129@gap.cgu.edu.tw

Chi-Chun Lai − *Department of Ophthalmology, Chang Gung Memorial Hospital, Linkou Main Branch, Taoyuan 333, Taiwan; Department of Ophthalmology, Chang Gung Memorial Hospital, Keelung 204, Taiwan;* orcid.org/0000-0001-9547-7212; Email: chichun.lai@gmail.com

Authors

Hung-Da Chou − *Department of Ophthalmology, Chang Gung Memorial Hospital, Linkou Main Branch, Taoyuan 333, Taiwan*

Chung-An Chen − *Department of Orthopaedic Surgery, Spine Section and Bone and Joint Research Center, Chang Gung Memorial Hospital, Taoyuan 333, Taiwan; School of Medicine, Chang Gung University, Taoyuan 333, Taiwan;* orcid.org/0000-0002-6647-3287

Hao-Yu Liu − *Department of Orthopaedic Surgery, Spine Section and Bone and Joint Research Center, Chang Gung Memorial Hospital, Taoyuan 333, Taiwan;* orcid.org/0000-0001-6722-9908

Shih-Jung Liu − *Department of Mechanical Engineering, Chang Gung University, Taoyuan 333, Taiwan;* orcid.org/0000-0003-2083-4865

Po-Liang Lai − *Department of Orthopaedic Surgery, Spine Section and Bone and Joint Research Center, Chang Gung Memorial Hospital, Taoyuan 333, Taiwan; School of Medicine, Chang Gung University, Taoyuan 333, Taiwan*

Wei-Chi Wu − *Department of Ophthalmology, Chang Gung Memorial Hospital, Linkou Main Branch, Taoyuan 333, Taiwan*

Yih-Shiou Hwang − *Department of Ophthalmology, Chang Gung Memorial Hospital, Linkou Main Branch, Taoyuan 333, Taiwan*

Kuan-Jen Chen − *Department of Ophthalmology, Chang Gung Memorial Hospital, Linkou Main Branch, Taoyuan 333, Taiwan*

Complete contact information is available at: https://pubs.acs.org/10.1021/acsomega.4c02842

Author Contributions

H.-D.C. and C.-A.C. contributed equally to this work. T.-T.T. and C.-C.L., conception and design of the work; H.-D.C., C.-A.C., H.-Y.L., S.-J.L., P.-L.L., W.-C.W., Y.-S.H., and K.-J.C., acquisition, analysis, and interpretation of data; H.-D.C., C.-A.C., and H.-Y.L., drafted the work and substantively revised it. All authors read and approved the final manuscript.

Funding

This study was partially supported by a Taiwan Ministry of Science and Technology Research grant [MOST110-2314-B-182A-020-MY3] and a Taiwan National Science and Technology Council grant [NSTC 112-2314-B-182-060, NSTC 112-2811-B-182-030]. The funding organizations had no role in the design or conduct of this research.

https://doi.org/10.1021/acsomega.4c02842
ACS Omega 2024, 9, 42147−42158

Notes

The authors declare no competing financial interest.

■ ACKNOWLEDGMENTS

We would like to thank the Laboratory Animal Center, Chang Gung Memorial Hospital, Linkou, Taiwan, for performing animal husbandry and care. We would like to thank the Microscopy Core Laboratory and Clinical Metabolomics Core Laboratory, Chang Gung Memorial Hospital, Linkou, for providing the SEM and NMR facilities. We thank Dr. Chih-Hsin Lin and the technical support provided by TMU Core Facility and Anton Paar Taiwan for the rheological analysis equipment. This manuscript was edited by Wallace Academic Editing.

■ REFERENCES

(1) Murphy, D. C.; Al-Zubaidy, M.; Lois, N.; Scott, N.; Steel, D. H.; Qu, J.; Zhao, M.; Sadda, S.; Manasa, S.; Agarwal, D.; et al. The Effect of Macular Hole Duration on Surgical Outcomes: An Individual Participant Data Study of Randomized Controlled Trials. *Ophthalmology* **2023**, *130* (2), 152−163.

(2) Chou, H. D.; Chong, Y. J.; Teh, W. M.; Chen, K. J.; Liu, L.; Chen, Y. P.; Yeung, L.; Hwang, Y. S.; Wu, W. C.; Lai, C. C. Nasal or Temporal Internal Limiting Membrane Flap Assisted by Sub-Perfluorocarbon Viscoelastic Injection for Macular Hole Repair. *Am. J. Ophthalmol.* **2021**, *223*, 296−305.

(3) Wu, A. L.; Liu, Y. T.; Chou, H. D.; Chuang, L. H.; Chen, K. J.; Chen, Y. P.; Liu, L.; Yeung, L.; Wang, N. K.; Hwang, Y. S.; et al. Role of Growth Factors And Internal Limiting Membrane Constituents In Müller Cell Migration. *Exp. Eye Res.* **2021**, *202*, 108352.

(4) Chou, H.-D.; Shiah, S.-G.; Chuang, L.-H.; Wu, W.-C.; Hwang, Y.-S.; Chen, K.-J.; Kang, E. Y.-C.; Yeung, L.; Nien, C.-Y.; Lai, C.-C. MicroRNA-152−3p and MicroRNA-196a-5p Are Downregulated When Müller Cells Are Promoted by Components of the Internal Limiting Membrane: Implications for Macular Hole Healing. *Int. J. Mol. Sci.* **2023**, *24* (24), 17188.

(5) Zhang, L.; Li, X.; Lin, X.; Wu, M. Nerve Growth Factor Promotes the Proliferation of Müller Cells Co-Cultured With Internal Limiting Membrane by Regulating Cell Cycle Via TRK-A/PI3K/AKT Pathway. *BMC Ophthalmol.* **2019**, *19* (1), 130.

(6) Arda, H.; Maier, M.; Schultheiß, M.; Haritoglou, C. Advances In Management Strategies For Large And Persistent Macular Hole: An Update. *Surv. Ophthalmol.* **2024**, *69* (4), 539−546.

(7) Chou, H. D.; Liu, L.; Wang, C. T.; Chen, K. J.; Wu, W. C.; Hwang, Y. S.; Chen, Y. P.; Kang, E. Y.; Chen, Y. H.; Yeung, L.; et al. Single-Layer Inverted Internal Limiting Membrane Flap Versus Conventional Peel for Small- or Medium-Sized Full-Thickness Macular Holes. *Am. J. Ophthalmol.* **2022**, *235*, 111−119.

(8) Lai, C.-C.; Chen, Y.-P.; Wang, N.-K.; Chuang, L.-H.; Liu, L.; Chen, K.-J.; Hwang, Y.-S.; Wu, W.-C.; Chen, T.-L. Vitrectomy with Internal Limiting Membrane Repositioning and Autologous Blood for Macular Hole Retinal Detachment in Highly Myopic Eyes. *Ophthalmology* **2015**, *122* (9), 1889−1898.

(9) Lai, C.-C.; Wu, A.-L.; Chou, H.-D.; Teh, W. M.; Chen, K.-J.; Chen, Y.-P.; Liu, L.; Hwang, Y.-S.; Wu, W.-C. Sub-Perfluoro-N-Octane Injection of Ocular Viscoelastic Device Assisted Inverted Internal Limiting Membrane Flap For Macular Hole Retinal Detachment Surgery: A Novel Technique. *BMC Ophthalmol.* **2020**, *20* (1), 116.

(10) Wang, Y.; Xu, Z.; Zhao, X.; Meng, L.; Yang, J.; Chen, Y. Therapeutic Effect Of Using Autologous Platelet Concentrate In Vitrectomy For Macular Hole: A Systematic Review and Meta-Analysis. *Retina* **2023**, *43* (11), 1833−1841.

(11) Cui, J.; Wang, H.; Shi, Q.; Sun, T.; Huang, Q.; Fukuda, T. Multicellular Co-Culture in Three-Dimensional Gelatin Methacryloyl Hydrogels for Liver Tissue Engineering. *Molecules* **2019**, *24* (9), 1762.

(12) Fan, C.; Ling, Y.; Deng, W.; Xue, J.; Sun, P.; Wang, D. A. A Novel Cell Encapsulatable Cryogel (CECG) With Macro-Porous Structures And High Permeability: A Three-Dimensional Cell Culture Scaffold For Enhanced Cell Adhesion And Proliferation. *Biomed. Mater.* **2019**, *14* (5), 055006.

(13) Campiglio, C. E.; Contessi Negrini, N.; Farè, S.; Draghi, L. Cross-Linking Strategies for Electrospun Gelatin Scaffolds. *Materials* **2019**, *12* (15), 2476.

(14) Shirahama, H.; Lee, B. H.; Tan, L. P.; Cho, N. J. Precise Tuning of Facile One-Pot Gelatin Methacryloyl (GelMA) Synthesis. *Sci. Rep.* **2016**, *6*, 31036.

(15) Klotz, B. J.; Gawlitta, D.; Rosenberg, A.; Malda, J.; Melchels, F. P. W. Gelatin-Methacryloyl Hydrogels: Towards Biofabrication-Based Tissue Repair. *Trends Biotechnol.* **2016**, *34* (5), 394−407.

(16) Benton, J. A.; DeForest, C. A.; Vivekanandan, V.; Anseth, K. S. Photocrosslinking of Gelatin Macromers to Synthesize Porous Hydrogels That Promote Valvular Interstitial Cell Function. *Tissue Eng., Part A* **2009**, *15*, 3221−3230.

(17) Lim, K. S.; Galarraga, J. H.; Cui, X.; Lindberg, G. C. J.; Burdick, J. A.; Woodfield, T. B. F. Fundamentals and Applications of Photo-Cross-Linking in Bioprinting. *Chem. Rev.* **2020**, *120* (19), 10662−10694.

(18) Pepelanova, I.; Kruppa, K.; Scheper, T.; Lavrentieva, A. Gelatin-Methacryloyl (GelMA) Hydrogels with Defined Degree of Functionalization as a Versatile Toolkit for 3D Cell Culture and Extrusion Bioprinting. *Bioengineering* **2018**, *5* (3), 55.

(19) Yue, K.; Trujillo-de Santiago, G.; Alvarez, M. M.; Tamayol, A.; Annabi, N.; Khademhosseini, A. Synthesis, Properties, And Biomedical Applications of Gelatin Methacryloyl (Gelma) Hydrogels. *Biomaterials* **2015**, *73*, 254−271.

(20) Vargas-Alfredo, N.; Munar-Bestard, M.; Ramis, J. M.; Monjo, M. Synthesis and Modification of Gelatin Methacryloyl (GelMA) with Antibacterial Quaternary Groups and Its Potential for Periodontal Applications. *Gels* **2022**, *8* (10), 630.

(21) Wang, X.; Liu, X.; Liu, W.; Liu, Y.; Li, A.; Qiu, D.; Zheng, X.; Gu, Q. 3D Bioprinting Microgels to Construct Implantable Vascular Tissue. *Cell Proliferation* **2023**, *56* (5), No. e13456.

(22) Shen, C.; Zhao, X.; Ren, Z.; Yang, B.; Wang, X.; Hu, A.; Hu, J. In Situ Formation of Injectable Gelatin Methacryloyl (GelMA) Hydrogels for Effective Intraocular Delivery of Triamcinolone Acetonide. *Int. J. Mol. Sci.* **2023**, *24* (5), 4957.

(23) Chen, F.; Qin, J.; Wu, P.; Gao, W.; Sun, G. Glucose-Responsive Antioxidant Hydrogel Accelerates Diabetic Wound Healing. *Adv. Healthcare Mater.* **2023**, *12* (21), 2300074.

(24) Xie, W.; Zhang, Y.; Zhang, J.; Chen, X.; Pan, J.; Zhu, X.; Pan, G. Dynamically Crosslinked Protien Hydrogel Composite As Multifunctional Wound Dressing For Cutaneous Infection. *Colloid Interface Sci. Commun.* **2022**, *50*, 100654.

(25) Alemdar, N.; Leijten, J.; Camci-Unal, G.; Hjortnaes, J.; Ribas, J.; Paul, A.; Mostafalu, P.; Gaharwar, A. K.; Qiu, Y.; Sonkusale, S.; et al. Oxygen-Generating Photo-Cross-Linkable Hydrogels Support Cardiac Progenitor Cell Survival by Reducing Hypoxia-Induced Necrosis. *ACS Biomater. Sci. Eng.* **2017**, *3* (9), 1964−1971.

(26) Chen, S.; Wang, Y.; Lai, J.; Tan, S.; Wang, M. Structure and Properties of Gelatin Methacryloyl (GelMA) Synthesized in Different Reaction Systems. *Biomacromolecules* **2023**, *24* (6), 2928−2941.

(27) Habeeb, A. F. S. A. Determination Of Free Amino Groups in Proteins By Trinitrobenzenesulfonic Acid. *Anal. Biochem.* **1966**, *14* (3), 328−336.

(28) Wang, Y.; Chen, Y.; Zheng, J.; Liu, L.; Zhang, Q. Three-Dimensional Printing Self-Healing Dynamic/Photocrosslinking Gelatin-Hyaluronic Acid Double-Network Hydrogel for Tissue Engineering. *ACS Omega* **2022**, *7* (14), 12076−12088.

(29) Shen, C.; Zhao, X.; Ren, Z.; Yang, B.; Wang, X.; Hu, A.; Hu, J. In Situ Formation of Injectable Gelatin Methacryloyl (GelMA) Hydrogels for Effective Intraocular Delivery of Triamcinolone Acetonide. *Int. J. Mol. Sci.* **2023**, *24* (5), 4957.

(30) Pfeffer, B. A.; Xu, L.; Porter, N. A.; Rao, S. R.; Fliesler, S. J. Differential Cytotoxic Effects of 7-Dehydrocholesterol-Derived Oxy-

https://doi.org/10.1021/acsomega.4c02842
ACS Omega 2024, 9, 42147−42158

sterols on Cultured Retina-Derived Cells: Dependence on Sterol Structure, Cell Type, And Density. *Exp. Eye Res.* **2016**, *145*, 297−316.
(31) Teshima, R.; Osawa, S.; Yoshikawa, M.; Kawano, Y.; Otsuka, H.; Hanawa, T. Low-Adhesion And Low-Swelling Hydrogel Based on Alginate And Carbonated Water to Prevent Temporary Dilation of Wound Sites. *Int. J. Biol. Macromol.* **2024**, *254*, 127928.
(32) Lei, Y.; Xiao, S.; Chen, S.; Zhang, H.; Li, H.; Lu, Y. N,N-dimethylformamide-induced acute hepatic failure: A case report and literature review. *Exp. Ther. Med.* **2017**, *14* (6), 5659−5663.
(33) Shukla, P.; Mitruka, M.; Pati, F. The effect of the synthetic route on the biophysiochemical properties of methacrylated gelatin (GelMA) based hydrogel for development of GelMA-based bioinks for 3D bioprinting applications. *Materialia* **2022**, *25*, 101542.
(34) Song, P.; Li, M.; Zhang, B.; Gui, X.; Han, Y.; Wang, L.; Zhou, W.; Guo, L.; Zhang, Z.; Li, Z.; et al. DLP fabricating of precision GelMA/HAp porous composite scaffold for bone tissue engineering application. *Composites, Part B* **2022**, *244*, 110163.
(35) Serafim, A.; Tucureanu, C.; Petre, D.-G.; Dragusin, D.-M.; Salageanu, A.; Van Vlierberghe, S.; Dubruel, P.; Stancu, I.-C. One-pot synthesis of superabsorbent hybrid hydrogels based on methacrylamide gelatin and polyacrylamide. Effortless control of hydrogel properties through composition design. *New J. Chem.* **2014**, *38* (7), 3112−3126.
(36) Jamshidifar, E.; Esfandyari-Manesh, M.; Motasadizadeh, H.; Naderizadeh, S.; Yourdkhani, A.; Samadi, N.; Dinarvand, R. Improvement of in vitro osteogenesis and anti-infection properties by GelMA scaffold containing levofloxacin nanoparticles and strontium microspheres for osteomyelitis. *J. Mater. Sci.* **2022**, *57* (28), 13603−13619.
(37) Wang, K.-Y.; Jin, X.-Y.; Ma, Y.-H.; Cai, W.-J.; Xiao, W.-Y.; Li, Z.-W.; Qi, X.; Ding, J. Injectable stress relaxation gelatin-based hydrogels with positive surface charge for adsorption of aggrecan and facile cartilage tissue regeneration. *J. Nanobiotechnol.* **2021**, *19* (1), 214.
(38) Tang, S.; Ma, H.; Tu, H.-C.; Wang, H.-R.; Lin, P.-C.; Anseth, K. S. Adaptable Fast Relaxing Boronate-Based Hydrogels for Probing Cell−Matrix Interactions. *Advanced Science* **2018**, *5* (9), 1800638.
(39) Liu, J.; Zhang, B.; Li, L.; Yin, J.; Fu, J. Additive-lathe 3D bioprinting of bilayered nerve conduits incorporated with supportive cells. *Bioact. Mater.* **2021**, *6* (1), 219−229.
(40) Moschos, M. M.; Chatziralli, I. P.; Sergentanis, T. N. Viscoat versus Visthesia during phacoemulsification cataract surgery: corneal and foveal changes. *BMC Ophthalmol.* **2011**, *11* (1), 9.
(41) Watanabe, I.; Hoshi, H.; Sato, M.; Suzuki, K. Rheological and Adhesive Properties to Identify Cohesive and Dispersive Ophthalmic Viscosurgical Devices. *Chem. Pharm. Bull.* **2019**, *67* (3), 277−283.
(42) Wang, Y.; Ma, M.; Wang, J.; Zhang, W.; Lu, W.; Gao, Y.; Zhang, B.; Guo, Y. Development of a Photo-Crosslinking, Biodegradable GelMA/PEGDA Hydrogel for Guided Bone Regeneration Materials. *Materials* **2018**, *11* (8), 1345.
(43) Cowan, C. S.; Renner, M.; De Gennaro, M.; Gross-Scherf, B.; Goldblum, D.; Hou, Y.; Munz, M.; Rodrigues, T. M.; Krol, J.; Szikra, T.; et al. Cell Types of the Human Retina and Its Organoids at Single-Cell Resolution. *Cell* **2020**, *182* (6), 1623−1640.e34.
(44) Tackenberg, M. A.; Tucker, B. A.; Swift, J. S.; Jiang, C.; Redenti, S.; Greenberg, K. P.; Flannery, J. G.; Reichenbach, A.; Young, M. J. Müller cell activation, proliferation and migration following laser injury. *Mol. Vision* **2009**, *15*, 1886−1896.
(45) Bringmann, A.; Iandiev, I.; Pannicke, T.; Wurm, A.; Hollborn, M.; Wiedemann, P.; Osborne, N. N.; Reichenbach, A. Cellular signaling and factors involved in Müller cell gliosis: neuroprotective and detrimental effects. *Prog. Retinal Eye Res.* **2009**, *28* (6), 423−451.
(46) Peña, J. S.; Vazquez, M. Harnessing the Neuroprotective Behaviors of Müller Glia for Retinal Repair. *Front. Biosci.* **2022**, *27* (6), 169.
(47) Tezel, G.; Li, L. Y.; Patil, R. V.; Wax, M. B. TNF-alpha and TNF-alpha receptor-1 in the retina of normal and glaucomatous eyes. *Invest. Ophthalmol. Visual Sci.* **2001**, *42* (8), 1787−1794.
(48) Torii, H.; Kurihara, T.; Seko, Y.; Negishi, K.; Ohnuma, K.; Inaba, T.; Kawashima, M.; Jiang, X.; Kondo, S.; Miyauchi, M.; et al. Violet Light Exposure Can. Be a Preventive Strategy Against Myopia Progression. *EBioMedicine* **2017**, *15*, 210−219.

https://doi.org/10.1021/acsomega.4c02842
ACS Omega 2024, 9, 42147−42158